2023

Enhanced Gene Transfection Efficacy and Safety Through Granular Hydrogel Mediated Gene Delivery Process

Jing Zhang
Nanjing Tech University, 30 Puzhu South Road, Nanjing, China

Zhonglei He
University College Dublin, Ireland

Yinghao Li
University College Dublin, Ireland

See next page for additional authors

Enhanced gene transfection efficacy and safety through granular hydrogel mediated gene delivery process

Jing Zhang [a 1], Zhonglei He [b c d 1], Yinghao Li [c], Yu Shen [a], Guanfu Wu [a], Laura Power [e], Rijian Song [c], Ming Zeng [f], Xianqing Wang [c], Irene Lara Sáez [c], Sigen A [c], Qian Xu [c], James F. Curtin [d g], Ziyi Yu [a], Wenxin Wang [b c]

[a]State Key Laboratory of Materials-Oriented Chemical Engineering, College of Chemical Engineering, Nanjing Tech University, 30 Puzhu South Road, Nanjing, 211816 China
[b]Research and Clinical Translation Center of Gene Medicine and Tissue Engineering, School of Public Health, Anhui University of Science and Technology, Huainan, 232001, China
[c]Charles Institute of Dermatology, School of Medicine, University College Dublin, Dublin, Ireland
[d]BioPlasma Research Group, School of Food Science and Environmental Health, Technological University Dublin, Dublin, Ireland
[e]Branca Bunús Ltd., Nova UCD, Belfield Innovation Park, University College Dublin, Dublin, Ireland
[f]Department of Dermatology, the First Affiliated Hospital of Jinan University, Guangzhou Overseas Chinese Hospital, Guangzhou 510630, China
[g]Faculty of Engineering and Built Environment, Technological University Dublin, Dublin, Ireland

[1]These authors contributed equally.

https://doi.org/10.1016/j.actbio.2023.04.041

Keywords

Gene therapy; Granular hydrogels; Controlled release; Gene delivery; Drug carriers

Corresponding Author

1. Wenxin Wang
   Research and Clinical Translation Center of Gene Medicine and Tissue Engineering, School of Public Health, Anhui University of Science and Technology, Huainan, 232001, China and Charles Institute of Dermatology, School of Medicine, University College Dublin, Dublin, Ireland
   Email: wwxph@aust.edu.cn and wenxin.wang@ucd.ie

2. Ziyi Yu
   State Key Laboratory of Materials-Oriented Chemical Engineering, College of Chemical Engineering, Nanjing Tech University, 30 Puzhu South Road, Nanjing, 211816 China,
   Email: ziyi.yu@njtech.edu.cn

Abstract

Although gene therapy has made great achievements in both laboratory research and clinical translation, there are still challenges such as limited control of drug pharmacokinetics, acute toxicity, poor tissue retention, insufficient efficacy, and inconsistent clinical translation. Herein, a gene therapy gel is formulated by directly redispersing polyplex nanoparticles into granular hydrogels without any gelation pre-treatment, which provides great convenience for storage, dosing and administration. In vitro studies have shown that use of granular hydrogels can regulate the gene drug release, reduce dose dependent toxicity and help improve transfection efficacy. Moreover, the developed gene therapy gel is easy to operate and can be directly used in vitro to evaluate its synergistic efficacy with various gene delivery systems. As such, it represents a major advance over many conventional excipient-based formulations, and new regulatory strategies for gene therapy may be inspired by it.

Statement of significance

A gene therapy gel is formulated by assembly of polyplex nanoparticles and granular hydrogels, which not only exhibits synergistic properties of controlled drug release, low cytotoxicity and high transfection efficacy, but provides great convenience for drug storage, dosing and administration. Moreover, depending on the applied load, the gene therapy gel can present either “solid-like” or “liquid-like” rheological response, allowing rapid drug application to lesion followed by efficient drug retention. As such, the gene therapy gel represents a major advance over many conventional excipient-based formulations and new gene delivery strategies may be inspired by it.

Graphical abstract

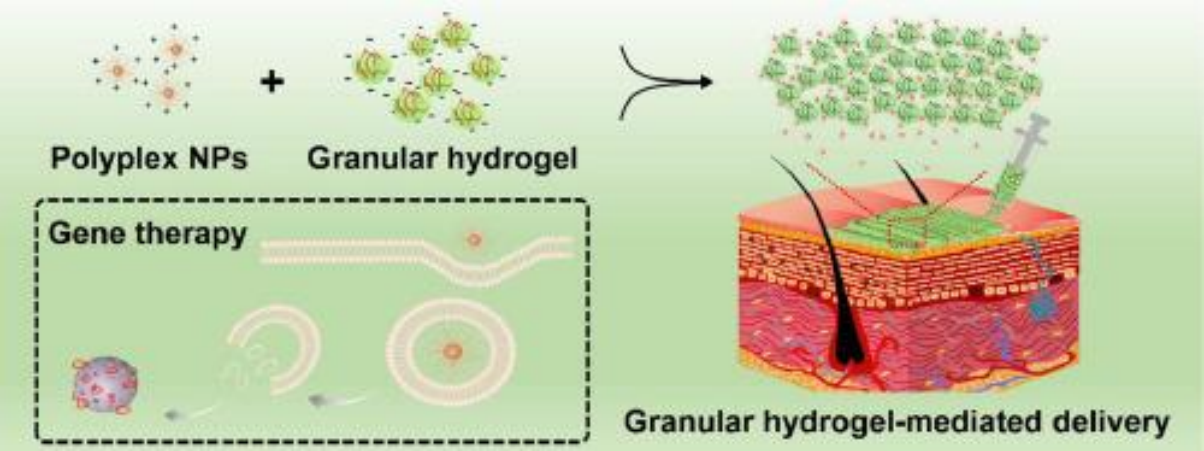

1. Introduction

Gene therapy has attracted increasing attention over the past few decades as a promising therapeutic approach to treat a variety of diseases, including inherited and acquired diseases. Despite the unprecedented success of COVID-19 vaccines, clinical translation of most gene therapy products is still hampered by the lack of safe and effective vectors and the need for minimally invasive routes of administration. In this respect, our team and many others have developed a series of non-viral vectors for gene therapy that promise to significantly improve transfection efficiency and safety [1,2]. Nevertheless, in most of the laboratory/preclinical studies, the genetic materials were dispensed in basic buffers and directly administrated via either topical applications for skin delivery or intratracheal instillation/nebulisation for lung delivery, without any additional excipients [3], [4], [5], [6], [7]. This often leads to limited control of drug pharmacokinetics, acute toxicity, poor tissue retention, insufficient efficacy and inconsistency in clinic translation.

Although several advanced topical or pulmonary administration methods have been described recently that could potentially eliminate the above-mentioned problems and improve the gene therapy efficacy [8], [9], [10], their widespread application may still be hampered by the adverse effects of complex preparation procedures, low patient compliance, and high manufacturing costs. For example, microneedle is complicated to manufacture, and its use can potentially cause additional harm to fragile, diseased skin tissues like those found in conditions such as epidermolysis bullosa and bullous pemphigoid. As a typical indication, recessive dystrophic epidermolysis bullosa (RDEB) is a rare genetic disorder caused by mutations in the gene COL7A1, which encodes type VII collagen that anchors the epidermis to the dermis [11]. RDEB patients' skin easily separates and forms blisters in response to minor trauma or friction, leading to open wounds and dermal exposure that increases the risk of infection, inflammation, scarring, and skin cancer. Thus, delivering gene therapy using hydrogels directly to the open wound may be an attractive option for RDEB patients due to its mild nature. Typical bulk hydrogel carriers have poor controllable porosity and high transfer invasiveness; in addition, harsh gel-forming conditions such as radiation, heat, or the use of organic solvents, may damage the nucleic acid structures or include toxic components that are difficult to remove afterwards [12]. On the other side, many traditional excipients, such as ethanol, glycerol, white petrolatum and honey, can be potentially formulated with polyplex nanoparticles, acting as penetration enhancers, thickeners or gelling agents to assist administration. However, quick and effective in vitro evaluation of excipient-vector interactions and drug efficacy are significantly hindered by the cytotoxicity of those excipients to monolayer cells caused by high osmotic pressure or the difficulty of handling viscous liquids/gels, which bring extra and heavy burden in the research of delivery formulations.

To address the issues, we propose herein a gene therapy gel formulated through direct assembly between granular hydrogels and vector-DNA polyplex nanoparticles. Granular hydrogels, also known as densely packed or jammed hydrogel microparticles (HMPs), exhibit unique properties, including shear-thinning, self-healing, modularity, etc., and are therefore widely used for drug delivery or as scaffolds that promote tissue regeneration [13], [14], [15]. Specifically, in this work, to prepare granular hydrogels, HMPs were first prepared by crushing a HA bulk hydrogel crosslinked by Michael type addition reaction between thiolate HA (SH HA) and acrylated HA (A-HA) through a defined micrometer-sized stainless-steel mesh (Fig. 1a). The resulting HMPs were then concentrated by centrifugation and mixed with the polyplex nanoparticles to produce the polyplex nanoparticles/granular hydrogel composites, i.e., the gene therapy gel. Unlike previously reported nondegradable carriers that are potentially deficient in biocompatibility and biosafety, herein, a hydrolyzable linear poly(β-amino ester)s (LPAEs, Fig. S1) polymer was selected as the gene delivery vector for proof of concept. Compared with nanoparticles-embedded preparations that lost their transfection ability, the gene therapy gel with surface adsorption of polyplex nanoparticles not only reduce the toxicity but improve the long-term efficacy. Combined with the fact that these gene therapy gels are shear thinning and injectable, they can further potentially be used as dressings or injectables (Fig. 1b). Overall, the results demonstrate that the developed gene therapy gel is easy to

formulate and manipulate, compatible with biodegradable vectors and can be directly incubated with cells for in vitro evaluation, thus with great advantages in formulation development and clinical translation.

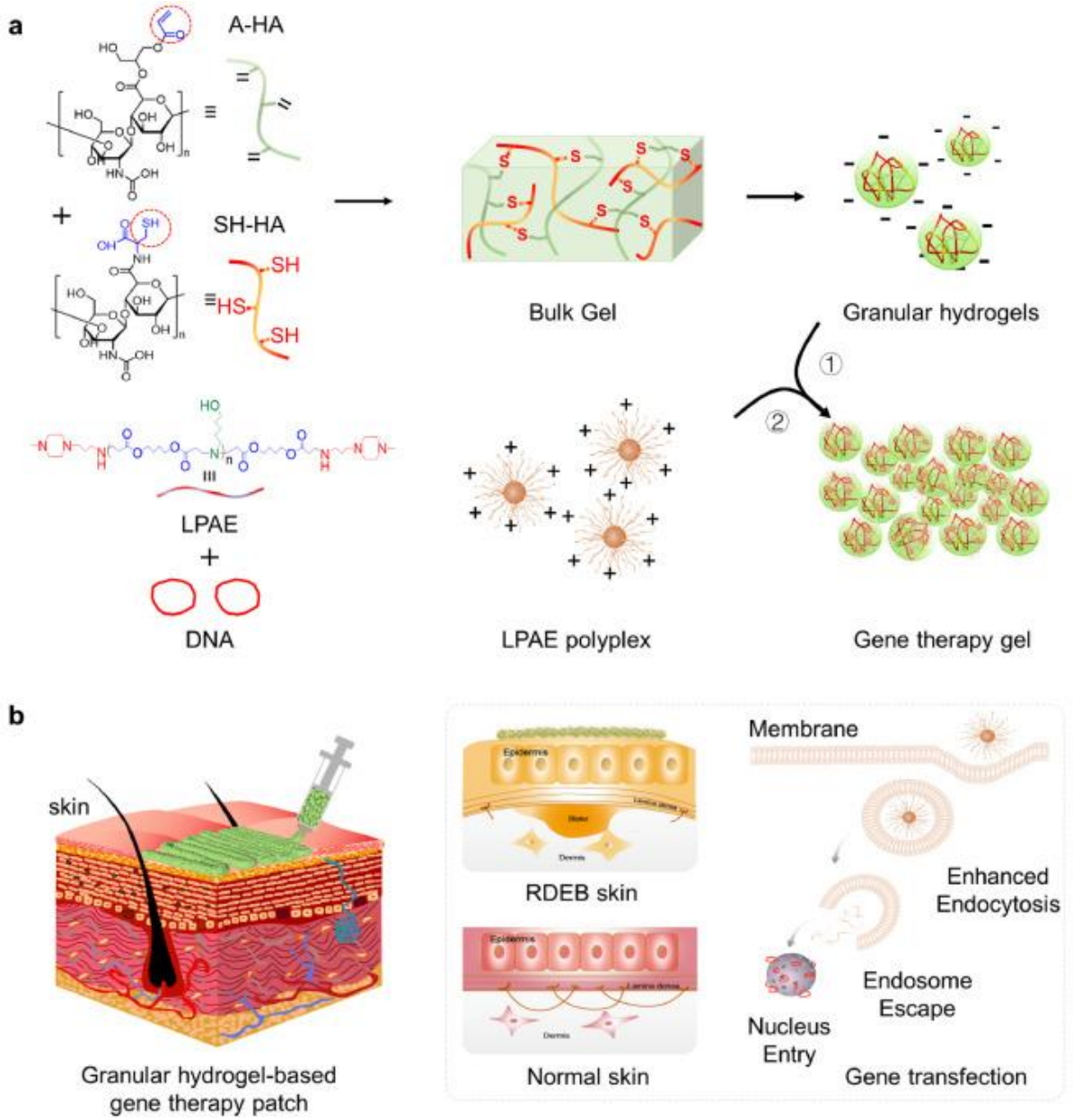

Fig. 1. HA granular hydrogel mediated gene delivery processes for enhanced gene transfection efficacy and safety. (a) Schematic illustration of the preparation of gene therapy gels by assembly between granular hydrogels and polyplex nanoparticles. (b) Schematic illustration of using the gene therapy gel as dressings to topically treat Recessive Dystrophic Epidermolysis Bullosa (RDEB).

2. Experimental section

2.1. Synthesis of LPAE polymers

LPAE was produced via a Michael addition reaction, where 1,4-butanediol diacrylate (BDA, 3.96 g) and 5-amino-1-pentanol (S5, 1.72 g) from Merck (Dublin, Ireland) were dissolved in 10 mL DMSO (Fisher Scientific, Dublin, Ireland). The mixture was then purged with argon for 15 min and the reaction took place at 90 °C. The progress of the reaction was monitored using Agilent 1260 Infinite gel permeation

chromatography (GPC) and nuclear magnetic resonance (NMR). Once the molecular weight (Mw) approached the target values (approximately 5k, 10k, 15k, and 20k), the reaction solution was diluted 10 times with DMSO and endcapped with an excess amount of 1-(3-aminopropyl)−4-methylpiperazine (E7, 1 g) purchased from Fisher Scientific (Dublin, Ireland) at room temperature for 48 h. Subsequently, the resulting polymer was precipitated into an acetone/diethyl ether mixed solution and dried under vacuum before being stored at −20 °C.

2.2. Characterization of LPAE polymers

Weight average molecular weight (Mw) and Mark-Houwink value of polymers were determined by GPC equipped with a refractive index detector (RI), a viscometer detector (VS DP) and a dual angle light scattering detector (LS 15° and LS 90°). To keep track of the Mw of the polymers throughout the polymerization procedure, 20 µL of the reaction mixture was taken at various time intervals, mixed with 1 mL of DMF, passed through a 0.2 µm filter, and subsequently measured by GPC. The GPC system consisted of two in-series columns which were eluted with DMF (Fisher Scientific, Dublin, Ireland) containing 0.1% LiBr (Merck, Dublin, Ireland) at a flow rate of 1 mL/min while maintaining a temperature of 60 °C. The chemical structure and composition of the polymers were verified by 1H NMR. LPAE was dissolved in CDCl3 (Merck, Dublin, Ireland) and the measurements were performed on a Varian Inova 400 MHz spectrometer, with the results reported in parts per million (ppm).

2.3. Preparation of the hydrogel microparticles (HMPs)

Fig. 1a and 2a illustrate the process for producing the gene therapy gel. The procedure involves two steps: bulk hydrogel synthesis and HMP preparation through crushing. Thiolated hyaluronic acid (SH HA, purity > 98%; Mw ≈ 220 kDa; 10% SD) and acrylated hyaluronic acid (A-HA, purity > 98%; Mw ≈ 220 kDa; 10% SD) were acquired from Blafar Ltd (Dublin, Ireland). In brief, SH HA and A-HA were separately dissolved in phosphate-buffered saline (PBS) at a concentration of 1.5% (w/v), respectively. The two solutions were mixed evenly in a 1:1 ratio and incubated at 37 °C for 24 h to form the HA bulk hydrogel. In the second step, the bulk HA hydrogel was extruded via stainless-steel meshes with different pore size ranges (Shaoxing Shangyu Huafeng Hardware Instrument Co., Ltd., China) to create HMPs of varying sizes. Unless otherwise stated, HMPs with an average diameter of 120 µm were used in subsequent experiments to ensure a large interstitial space between HMPs and the diffusion of the polyplex nanoparticles therein.

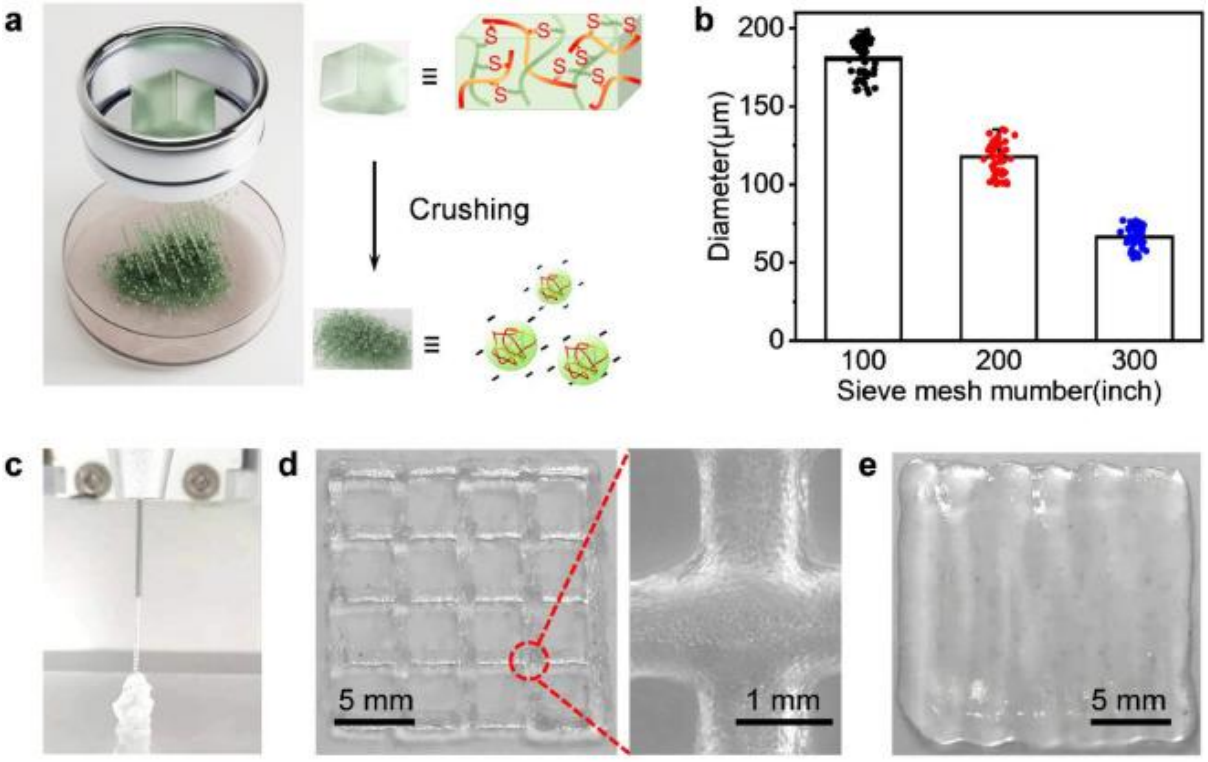

Fig. 2. Preparation of HA granular hydrogels. (a) HMPs were prepared by crushing of the crosslinked HA hydrogel through a defined micrometer-sized stainless-steel mesh. (b) The HMP sizes were easily adjusted by changing the mesh size. The average diameters of the HMPs were obtained by measuring about 50 particles for each sample. (c) Photograph of the granular hydrogel filament while it is extruded from a 26 G conical nozzle. Photographs of the grid printed by (d) the granular hydrogel and (e) gene therapy gel.

2.4. Polyplex nanoparticle synthesis, gene therapy gel formulation, and release analysis

A stock solution of LPAE was prepared by dissolving it in DMSO at a concentration of 100 mg/mL, and was stored at −20 °C. DNA, on the other hand, was dissolved in pure water at a concentration of 1 mg/mL and stored at −20 °C as well. A working solution of 25 mM sodium acetate (NaOAc, 3 M) buffer (pH 5.2), purchased from Merck (Dublin, Ireland), was prepared by diluting it in deionized water. To prepare the polyplex nanoparticles, the stock solutions of DNA and LPAE were first diluted in 25 mM NaOAc buffer to final concentrations of 0.1 mg/mL and 2 mg/mL, respectively. The solutions were mixed in equal volume by vortexing for 10 s and incubated for another 5 min at room temperature to obtain the final polyplex nanoparticles with a polymer:DNA weight ratio of 20:1. Similarly, polyplexes with different polymer:DNA weight ratios (15:1, 30:1, and 40:1) were prepared using the same method. Once the dispersion was prepared, sucrose was added to attain a concentration of 10% (w/v), and the resulting mixture was frozen at −80 °C for an hour. The samples were then subjected to lyophilization using a Christ Alpha 1–2 LDplus Freeze-Dryer (Dublin, Ireland) at a temperature of −55 °C for 24 h.

To produce granular hydrogels with a high packing density, HMPs suspended in PBS underwent centrifugation at 200 x g for 5 min, and the supernatant was replaced with complete culture medium. This step was repeated five times to ensure sufficient fluid replacement between the HMPs. The

packing density of the resulting granular hydrogel was further adjusted by adding complete media. Unless otherwise stated, granular hydrogels with a solid content of 0.8 wt% were used in subsequent experiments. Next, a specified amount of lyophilized polyplex nanoparticles was mixed with the granular hydrogel to create the gene therapy gel for cell transfection. If not specifically indicated, the gene therapy gel utilized in this study was created by mixing lyophilized polyplex nanoparticles with granular hydrogel to achieve a DNA concentration of 5 μg/mL. Furthermore, to enclose the polyplex nanoparticles within HMP, the lyophilized polyplex nanoparticles were included in the combination of A-HA and SH HA before crosslinking. Afterward, the HA bulk hydrogel that was created was transformed into HMP using the crushing method mentioned earlier.

The tracking and release analysis were performed by fluorescently labeling the DNA within the polyplex nanoparticles with Cy3, in accordance with the standard commercial protocol of the Label IT kit (Mirus, Madison, WI, USA). The resulting Cy3-DNA/LPAE polyplex nanoparticles were then prepared using the previously mentioned method and employed in a standard manner. For release studies, the Cy3-DNA/LPAE polyplex nanoparticles were mixed with 1 mL of granular hydrogel to achieve a DNA concentration of 5 μg/mL. Subsequently, 0.5 mL of PBS was added to the mixture and incubated at 37 °C. At each time point, three PBS suspension samples, each with a volume of 0.1 mL, were examined for Cy5 signal using a SpectraMax M3 multi-plate reader (Molecular Devices, San Jose, CA, USA). To establish the baseline and the maximum signal, untreated PBS and 1.5 mL of PBS containing 5 μg DNA formed polyplex were used as blank and 100%, respectively.

2.5. Cell culture

The COS7 cell line, derived from immortalized African green monkey kidney fibroblasts, along with the HEK293 cell line from immortalized human embryonic kidneys, and the A549 cell line from human Caucasian lung carcinoma, were grown in full culture media consisting of Dulbecco's modified Eagle Medium supplemented with 10% fetal bovine serum and 1% Penicillin/Streptomycin (Merck, Dublin, Ireland). The cells were maintained at 37 °C with 5% CO2 in a humid incubator under typical cell culture conditions. The immortalized RDEB keratinocytes (RDEBK) were generously provided by Prof. Fernando Larcher from Centro de Investigaciones Energéticas, Medioambientales y Tecnológicas-CIEMAT, Madrid, Spain. The cells were cultured using standard techniques for cell culture in keratinocyte growth complete FAD medium (KCa), and were maintained in a humidified incubator at 37 °C with 5% CO2.

2.6. Cell transfection, GFP expression and cell viability

The transfection efficiency of polyplex nanoparticles was assessed using gWiz-GFP plasmids obtained from Aldevron (North Dakota, USA) and the plasmid named pcDNA3.1C7 which contains a human COL7A1 gene sequence, was kindly provided by Dr A. South (Thomas Jefferson University, Department of Dermatology and Cutaneous Biology, Philadelphia, PA, USA). The polyplex nanoparticles were dispersed either directly in culture media (referred to as free LPAE Polyplex) or in granular hydrogels (referred to as Gene therapy gel) or encapsulated in HMPs (referred to as Trapped therapy gel). To assess the effectiveness of transfection, cells were plated in 96-well plates with a density of 1 × 104 cells in 100 μL of media, 24 h before the transfection process. Then, free LPAE Polyplex or Gene therapy gel or Trapped therapy gel, each containing 0.5 μg of DNA plasmid equivalent, was added to each well. After a 48-hour period post-transfection, the expression of GFP in each well was observed and recorded under a fluorescent microscope (Olympus IX81, Dublin, Ireland). The integrated density (IntDen) of GFP in each image was subsequently measured using ImageJ. Cell transfection using jetPEI

(Polyplus, Illkirch, France) and Lipofectamine 3000 (Lipo3k, Thermal Fisher, Dublin, Ireland) was performed following the standard protocol provided by the manufacturers. The nanoparticles were prepared with jetPEI:DNA ratio of 2:1 (µL/µg) and Lipo3k:DNA ratio of 3:1 (µL/µg), respectively. Cell viability was assessed using a standard Alamar Blue assay (Thermal Fisher, Dublin, Ireland), while GFP expression was determined by measuring the integrated density of each image. Both cell viability and GFP expression were measured in at least triplicate.

For the long-term GFP expression study, HEK293 cells were seeded in a 24-well plate at an initial density of 1 × 106 cells/mL in growth medium. After 24 h, the cells were transfected using various conditions as indicated. The cells were then sub-cultured every two days at a 1:5 split ratio. The stability and duration of GFP expression after transfection were assessed by observing the cells at regular intervals under a fluorescence microscope. The initial observation was made 48 h post-transfection, followed by subsequent observations 24 h after each subculture.

The live/dead staining was performed on the COS7 cell line after being exposed to different volume ratios of granular hydrogel to culture media, ranging from 0% to 40%. Cells were seeded at a density of 1 × 104 cells/well in a 96-well plate and allowed to adhere overnight. Subsequently, the cells were treated with granular hydrogels in culture media. To assess cell viability, the LIVE/DEAD™ Viability/Cytotoxicity Kit for mammalian cells (Thermo Fisher, Dublin, Ireland) was employed. The assay involved removal of the previous media after 48 h of incubation with the test compounds, followed by addition of a staining PBS solution containing 2 µM of Calcein-AM and 4 µM of ethidium homodimer-1 (EthD-1). The mixture was then incubated at room temperature for 30 min prior to fluorescent imaging (excitation/emission: Calcein-AM 494/517 nm; EthD-1 528/617 nm).

Intracellular imaging of Cy3-DNA/LPAE polyplex nanoparticles was achieved by transfecting cells using the standard protocol. Four hours post-transfection, the cells were rinsed three times with PBS and then incubated in pre-warmed PBS with NucBlue™ Live ReadyProbes™ Reagent (Hoechst 33,342, Thermo Fisher Scientific, Dublin, Ireland) for 20 min using the standard commercial protocol. Afterwards, the fluorescence imaging was conducted using an Olympus IX83 microscope (Olympus, Tokyo, Japan).

2.7. Immunocytochemistry

48-well plates containing 9 mm coverslips were used to pre-seed RDEBK cells. After 24 h, all cells were transfected with the specified conditions. Following a 72-hour post-transfection period, the coverslips were fixed using ice-cold acetone:methanol for 20 min at −20 °C, after which they were washed three times with ice-cold PBS. Non-specific binding sites were then blocked using 3% bovine serum albumin (BSA, Sigma Aldrich, Dublin, Ireland), and the cells were subsequently incubated with a rabbit anti-C7 primary antibody (provided by Dr. Alexander Nyström) at a dilution of 1:5000 overnight at 4 °C. After washing the coverslips three more times with PBS, they were incubated with an AlexaFluor™ 568-labeled secondary antibody (A-11,031) (Thermo Fisher Scientific, Dublin, Ireland) at a dilution of 1:800 for 1 hour at room temperature. Finally, the coverslips were mounted on microscope slides using Fluoroshield (Abcam, Dublin, Ireland) mounting medium containing DAPI and imaged using the Olympus IX83 microscope.

2.8. Flow cytometric analysis

The RDEBK cells were cultured and transfected as previously described in a 24 well plate format. After 48 h of transfection, the cells were rinsed twice with PBS and then detached by incubating them with pre-warmed 0.25% trypsin for 10 min. The trypsin activity was subsequently neutralized by adding culture media containing 10% FBS, and all the liquid from each step was collected into a single tube to obtain all the suspended or adherent, living, and dead cells. The living and dead cells were then collected by centrifugation at 300 × g for 3 min, and resuspended in 0.3 mL of PBS. The transfection efficiency and cell density were evaluated using the CytoFLEX Flow Cytometer (Beckman Coulter Life Sciences, Indianapolis, IN, USA) and the CytExpert software.

2.9. Growth rate and doubling time

HEK293 cells were seeded in 24-well plates at a density of 100,000 cells/mL. After 24 h, different conditions were used to transfect the cells, and the cell density was considered as 100,000 cells/mL at the starting point (0 h). For each indicated time point, three wells were selected for each condition. The culture medium was removed from the selected wells using a sterile pipette, and the cells were washed with PBS before being treated with trypsin to detach them. The trypsin was neutralized with full medium, and the cell suspension was counted using a hemocytometer according to the standard protocol to determine the cell density. The cell number (density) and time of the cell count were recorded for each time point, and the growth curve was generated by plotting the cell density versus time. To determine the growth rate and doubling time of the cells, the following equation was employed: growth rate = natural logarithm of the ratio of the number of cells at time t (N(t)) to the number of cells at time 0 (N(0)), divided by the time interval (t) between the two measurements; doubling time (DT) was calculated as the natural logarithm of 2 divided by the growth rate.

2.10. Statistical analysis

Each experiment was conducted in at least triplicate ($n \geq 3$). All data are presented as mean ± standard deviation. Statistical differences were analyzed with GraphPad Prism 5. The unpaired Student's t-test was used to test statistical difference between two measurements. One-way ANOVA test was used to test statistical difference between sets of measurements. p-Values below 0.05 were considered significant.

3. Results and discussion

3.1. Preparation of the gene therapy gel and its favorable rheological properties

HA, a highly hydrophilic polysaccharide, is chosen here for the preparation of the granular hydrogel because it occurs naturally as a fundamental component of the human extracellular matrix (ECM) and has been widely shown to promote wound healing and enhance the transdermal penetration of nanostructures [16,17]. Specifically, SH HA and A-HA were first prepared (Fig. 1a) and bulk HA hydrogels were then formed through Michael addition reaction of double bonds and free thiol groups introduced in their structures. Compared with physical crosslinking, chemical crosslinking between endogenous groups in HAs not only reduces the material cytotoxicity by consuming the excess reactive

groups in HAs (Fig. S2) but improves the mechanical properties of the formed gel. The HMPs constituting the granular hydrogel were fabricated by crushing the HA bulk hydrogel through a defined micron-scale stainless steel mesh, and changing the mesh size allowed us to easily adjust their sizes (Fig. 2a,b, and Fig. S3). Compared with other HMP preparation methods such as microfluidics [18,19], suspension emulsion polymerization [20,21], inkjet printing [22,23], etc., the preparation method adopted in this work has advantages of low cost, high yield, and does not involve the use of any potentially toxic dispersants or purification reagents, which is thus more conducive to clinical translation. The HMP dispersion was then concentrated by centrifugation and the supernatant was removed to obtain the final granular hydrogel to load polyplex nanoparticles to form the gene therapy gel.

As Fig. 2c shows, the gene therapy gels are injectable, allowing arbitrary 2D patterns to be fabricated by an extrusion 3D printer coupled with a 26-gage syringe needle. Due to the weak physical interactions between the HMPs, the printed lattice will gradually collapse (high-resolution image on the right side of Fig. 2d), and under weak external shear stress, a uniform coating can be attained (Fig. 2e). Given that the gene therapy gel in this study is intended for the treatment of recessive dystrophic epidermolysis bullosa (RDEB), a severe skin blistering condition that results from genetic mutations in the COL7A1 gene (as illustrated in Fig. 1b), the favourable characteristics discussed earlier, such as injectability and uniformity, make gene therapy gels an advantageous option for topical treatment as an alternative soft dosage form. Moreover, compared to conventional ointment or cream formulations, the gene therapy formulation containing only HA and polyplex nanoparticles is simple and additive-free, so it is less likely to cause skin sensitivity or irritation. Additionally, the administration of the gene therapy gel only involves simple redispersion of polyplex nanoparticles in granular hydrogel without any pre-treatment for gelation, providing great convenience for storage, dosing, and administration in practical use.

Previous studies have shown that the rheological properties of soft dosage drugs significantly affect drug release, drug therapeutic efficacy and consumer requirements (extrusion from tube, convenience, and ease of lubrication on the skin). Fig. 3 details the rheological properties of the gene therapy gel. The oscillatory amplitude sweep measurement results are first illustrated in Fig. 3a,b, which depicts the variation of dynamic storage modulus (G′) and loss modulus (G″) with shear strain (γ). These tests are performed in the strain range that covers both small and large amplitude deformation regimes for a rational understanding of the linear viscoelastic (LVE) and non-LVE behavior of the gene therapy gels. The constant plateau values at low strain indicate that they exhibit a primarily solid-like elastic response in this strain range. At higher deformation amplitudes, G′ decreases because of the collapse of the HMP jamming structure. Eventually, G′/G″ cross-over happens at the cross-over strain, indicating a solid-like to liquid-like transition, and the gene therapy gels demonstrate a viscosity-dominant rheological response. It should be noted that the G″ curves do not fall constantly when the deformation is increased beyond the LVE range. They show one peak in the partial range indicating the increasing portion of deformation energy which is spent to change the HMP jamming structure of gene therapy gels.

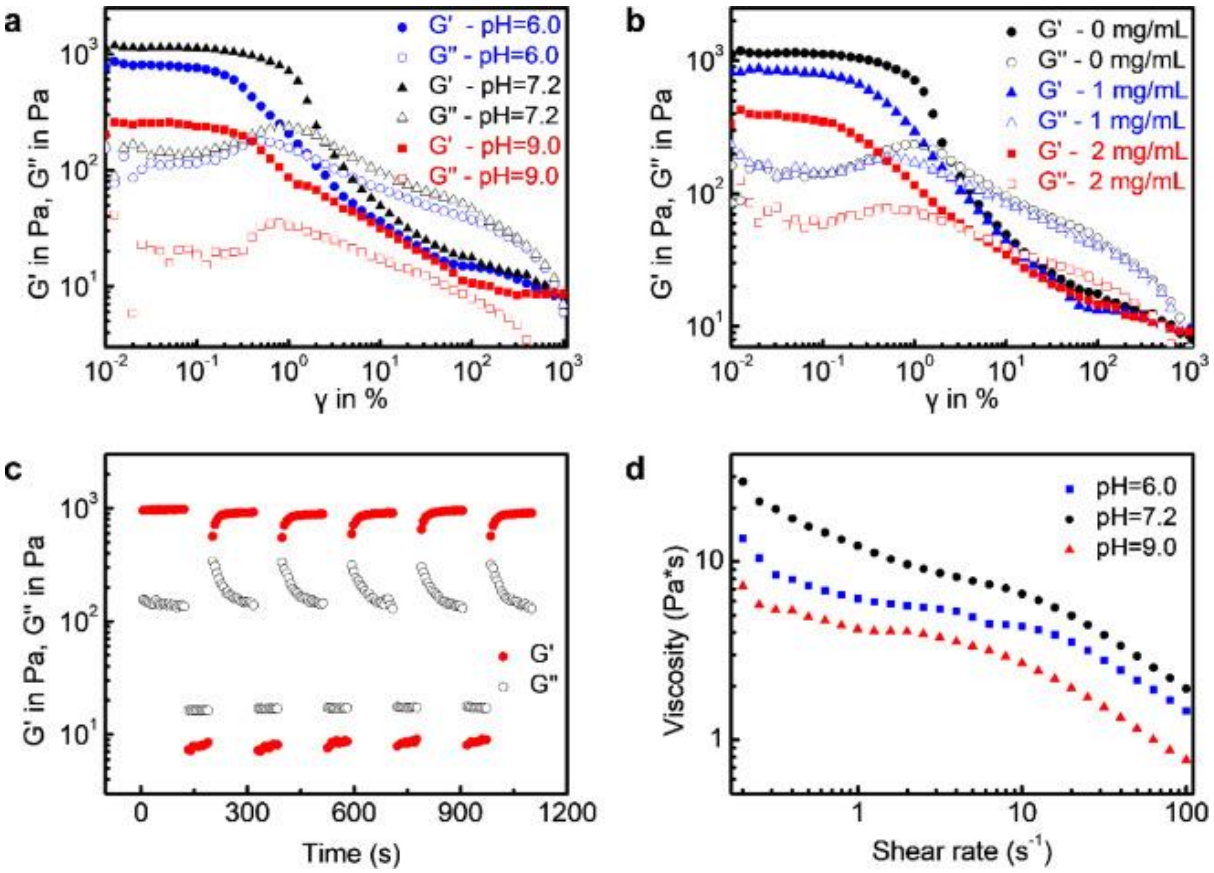

Fig. 3. Rheological characterizations of the gene therapy gels. Amplitude sweep test results of gene therapy gels (a) at different pH and (b) with varying concentrations of lyophilized polyplex nanoparticles, which included glucose as a lyoprotectant. Strain sweeps were performed with oscillation strain amplitudes of 0.01 - 1000% at a constant angular frequency of 1 Hz. (c) G′ and G′′ recovery of the gene therapy gel after subjecting the gene therapy gels to alternating high strain (1000%) and low strain condition (0.1%). (d) Viscosity of the gene therapy gels at increased shear rate by continuous flow experiment, indicating the shear-thinning characteristic.

The effect of the polyplex nanoparticle concentration and pH on the rheological properties of gene therapy gels is also investigated. As shown in Fig. 3a, when the pH value deviates from neutral conditions, G' decreases significantly. Likewise, as more and more lyophilized polyplex nanoparticles are introduced into the gene therapy gel, the G' value shows a similar downward trend (Fig. 3b). These features indicate that the introduction of polyplex nanoparticles and the local acidic environment would make the gene therapy gel softer and more prone to deformation under external forces. Next, to study the self-healing behavior of the gene therapy gel, an oscillatory strain alternation between 1000% and 0.1% was applied at the same frequency (1 Hz). As shown in Fig. 3c, for a high magnitude strain (1000%), the gene therapy gel exhibits shear-thinning, as G″ > G′, indicating a sol state. Moreover, when the strain is switched to a low magnitude strain (0.1%), the sol exhibits quick recovery to gel state, indicating self-healing behavior. Additionally, in a continuous flow experiment, we measured the instantaneous viscosity modulus under a controlled frequency of 1 Hz and a wide range of shear rates from 0.01 to 100 s−1. As shown in Fig. 3d, the gene therapy gels show good shear-thinning performance. The characteristic indicates that the gene therapy gel become viscous and easy to flow under the action of external shear force, which is beneficial to spreading on the skin; when the external force is removed, the gel immediately restores its elasticity, realizing local drug retention. The perfect mechanical properties including shear thinning and self-healing have brought broad application prospects for gene therapy gels as soft dosages.

3.2. Gene therapy gel mediated delivery to promote enhanced transfection efficacy and reduced cytotoxicity

To date, only a limited number of studies have utilized degradable carriers for hydrogel-mediated gene delivery [24,25]. Instead, the majority of research in this area has employed non-degradable or slowly degradable vectors, such as PEI [26,27], PAMAM dendrimers [28,29], and chitosan [30,31]. This is because the high-water content of the hydrogel environment may cause vector degradation, which could significantly diminish their efficacy. However, we reasoned that highly degradable vectors for gene delivery could be better alternatives for clinical translation, and tuning loading methods might allow them to be modulated by hydrogels and further enable gene therapy. To achieve this, granular hydrogels are selected as the mediator for controlled release while biodegradable LPAE polymers synthesized by Michael addition between amines and acrylate monomers (Fig. S1) are selected as the DNA vectors. LPAEs are positive charged polymers that can condense negatively charged nucleic acids after protonation [32] and can be hydrolysed spontaneously in aqueous solution or accelerated by esterase. The high safety profile makes LPAEs promising for clinical translation and thus differs from previously described non-degradable or slowly degrading vectors [27,32]. Moreover, LPAEs and their analogues can be readily synthesised without by-products, using many commercially available amine and acrylate monomers, and thus possess a large structural library from which numerous PAEs candidates with potent in vitro and in vivo transfection efficacy have been screened and optimised [33], [34], [35]. In addition to topical skin application, delivery of drugs or genes via the pulmonary route is also very attractive due to the sufficient blood supply and thin alveolar epithelial lining of the large surface area of the lungs [12], where many lung-related fatal diseases occur awaiting new and effective treatments. Accordingly, we use adenocarcinoma human alveolar basal epithelial cells (A549) and keratinocyte cell lines derived from severe generalized recessive epidermolysis bullosa patients for transfection experiments here.

In this study, two methods were utilized to integrate LPAE-pDNA polyplex nanoparticles into HA granular hydrogels. The initial approach, surface loading, required mixing lyophilized polyplex nanoparticles and HA granular hydrogel directly to produce a gene therapy gel (Fig. S4). The second technique, encapsulation, involved introducing lyophilized polyplex nanoparticles into the HMP matrix that comprises the HA granular hydrogel, resulting in a trapped therapy gel. The obtained gels were then incubated with monolayer A549 cells for 1, 4 or 48 h and then replaced with fresh culture media. As depicted in Fig. 4a-c, although the gene therapy gel had relatively lower efficacy compared to free LPAE polyplex for the shorter-term exposure groups (1 and 4 h), it exhibited pronounced levels of GFP expression with 48-h action of the gene therapy gel. Furthermore, the gene therapy gel showed negligible toxicity in compared to free LPAE polyplex and commercial vectors including jetPEI and Lipofectamine 3000 (Lipo3k) (Fig. 4b,e). The reason behind this outcome is that, although the initial electrostatic adsorption causes a decline in drug concentration (as demonstrated in Fig. S5) leading to a decrease in GFP expression, the toxicity of the polyplex nanoparticles, which is dependent on the dosage, is reduced. Moreover, the nanoparticles that are attached are efficiently released in the following hours, which leads to sustained transfection effectiveness. Hence, the optimized release process of the gene therapy gel achieves a balance between efficiency and cytotoxicity. Additionally, long-term studies on the growth rate and GFP expression of the transfected cells were conducted (Fig. S6), which further confirms the lower cytotoxicity and long-term efficacy of the gene therapy gel.

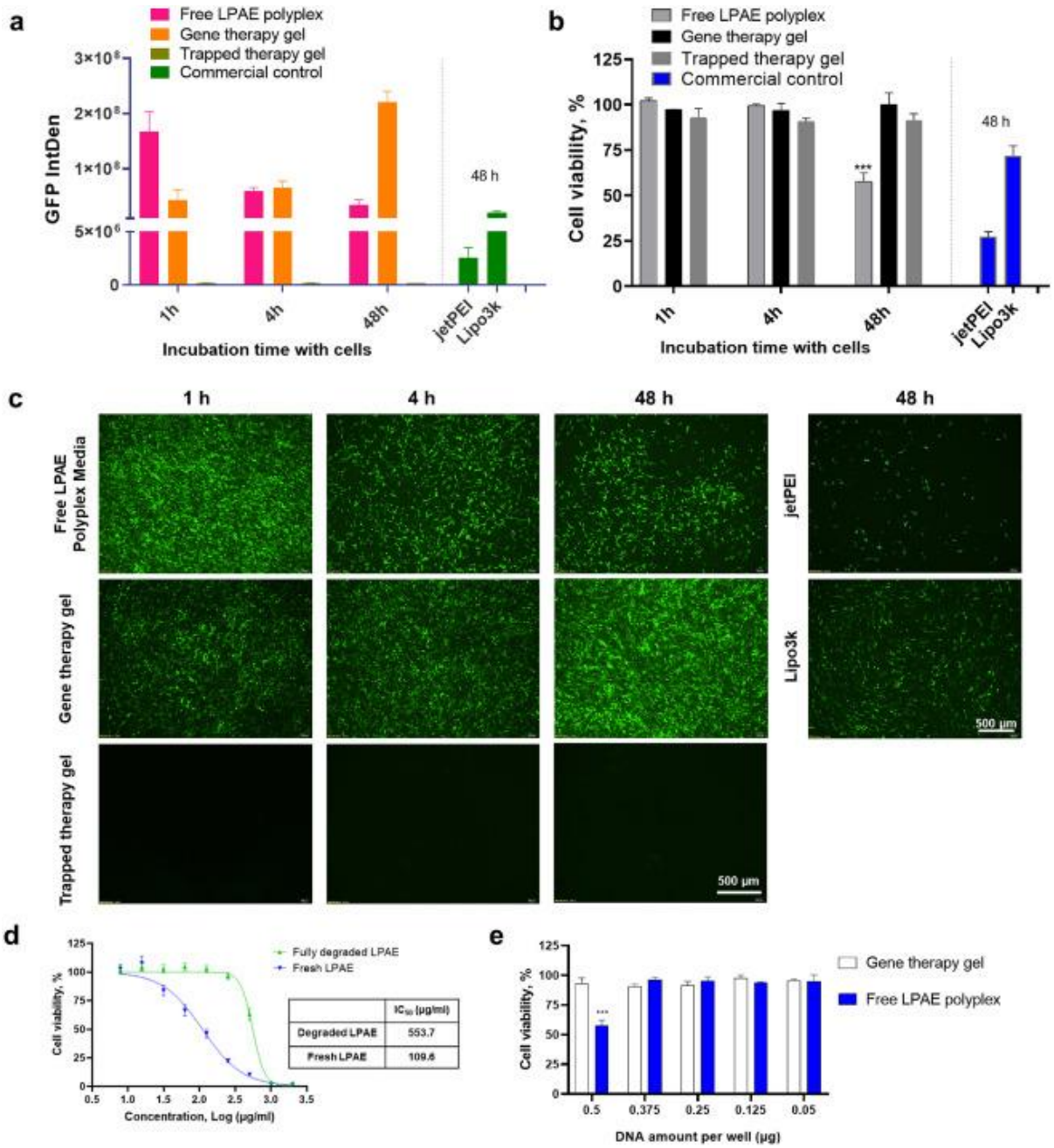

Fig. 4. The transfection efficacy can be optimized, and the cytotoxicity reduced by using a gene therapy gel that gradually releases LPAE-DNA polyplex. (a) The comparison of green fluorescent protein (GFP) expression in A549 cells transfected with various products, including free LPAE polyplex, gene therapy gel, and trapped therapy gel, as well as commercially available products like jetPET and Lipo3k. (b) The viability of transfected A549 cells. (c) To compare the results, representative images of the transfected A549 cells were displayed together. (d) Dose-response curves and IC50 values of both fully degraded and fresh LPAE polymers. (e) The impact of high doses of LPAE-DNA polyplex nanoparticles on cell viability, as well as the preventive effect of gene therapy gels on the reduction of cell viability caused by these nanoparticles.

The cytotoxicity of LPAE and its degradation productions were also tested. Fig. 4d shows that LPAE fully hydrolysed by dissolving in water and incubating at 37 °C for 4 h is less cytotoxic with an IC50 value of 553.7 µg/mL compared to fresh LPAE (109.6 µg/mL), which also confirms that giving a fix dose at a relatively longer term shall assist reduction of toxicity of LPAE-DNA polyplex nanoparticles. On the other hand, the trapped therapy gel failed to transfect A549 cells (Fig. 4a-c). This may be due to the

fact that the HA hydrogels degrade slowly, causing most of the polyplex nanoparticles to remain trapped and unable to be released until the hydrogel breaks down. This is consistent with previous research that has used non- degradable or slow-degradable vectors for gene drug sustained release. Consequently, gene therapy gels are a preferable formulation option due to their ability to achieve minimal toxicity at this dosage level while also possessing sustained release properties.

Next, RDEB keratinocytes (RDEBK) carrying a highly recurrent COL7A1 homozygous mutation as an ideal model for RDEB treatment [36] were transfected with similar conditions. It demonstrates an alike trend: for the short-term exposure groups (1 hour and 4 h), the gene therapy gel showed relatively low efficacy compared to free LPAE polyplex, whereas it showed significant GFP expression levels 48 h after the gene therapy gel treatment. (Fig. 5a-c). For flow cytometry analysis, three transfection conditions were selected, including the free LPAE polyplex group, the gene therapy gel group, and Lipo 3k group, in comparison to the untreated control group (Fig. S7a). Interestingly, all transfected groups showed similar mean and median fluorescence intensity of GFP and had high percentages of GFP-positive cells (Fig. S7a-c). The Lipo 3k group had slightly higher median GFP compared to the other two groups (Fig. S7c). However, when all dead and alive cells were collected and suspended in the same amount of cytometry buffer, the cell number (singlet events)/µL was significantly lower in the LPAE polyplex group and the Lipo 3k group than in the gene therapy gel group, which was consistent with previous cell viability analysis (Fig. 4b and Fig. S7d). Based on image analysis, it appears that the gene therapy gel-transfected cells had higher GFP expression, likely due to a significantly higher total signal from more viable and transfected cells. While the Lipo 3k-transfected cells showed high median GFP expression, the use of this cationic lipid-based reagent may compromise biocompatibility despite its potency. Furthermore, a stability test was performed on the free polyplex nanoparticles (Fig. 5d), which indicated that a pre-incubation time of less than 4 h at 37 °C led to higher efficacy and reduced cytotoxicity, while a pre-incubation time of more than 4 h resulted in a rapid decline in transfection efficacy. The cause of this decline requires further investigation. These findings, combined with the fact that most of the polyplex nanoparticles can be released from the gene therapy gel within the first 4 h (Fig. S5), suggest that gene therapy formulations could be a highly promising alternative for achieving enhanced gene transfection efficacy and safety.

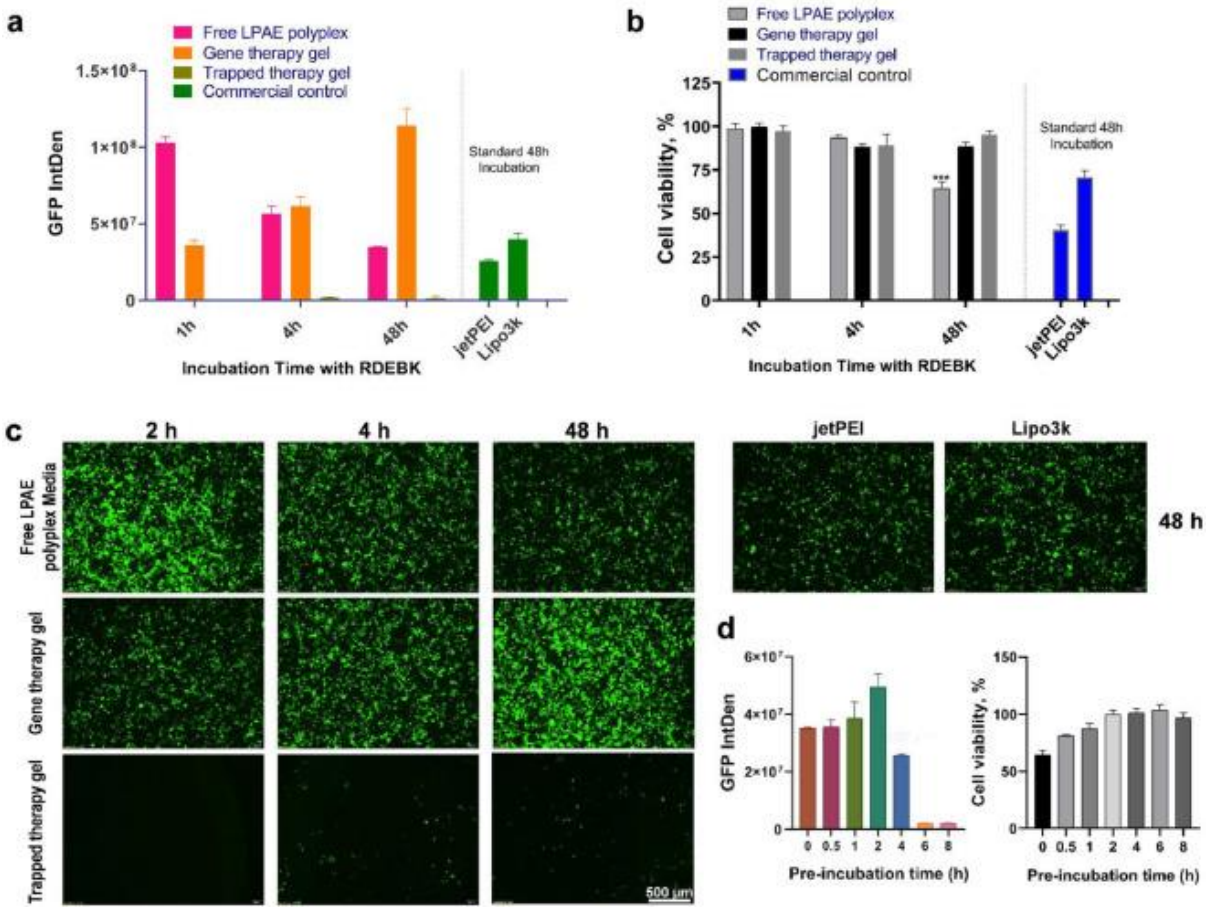

Fig. 5. The enhanced transfection efficacy and decreased cytotoxicity of gene therapy gels in RDEBK cells. (a) The GFP expression of RDEBK cells transfected by free LPAE polyplex, gene therapy gel, and trapped therapy gel, as well as commercially available products like jetPET and Lipo3k. (b) The viability of transfected cells. (c) Representative images were presented together for comparison. (d) Stability tests of free LPAE polyplex nanoparticles. One-way ANOVA test was used to identify the significance (*** $p < 0.001$).

Although gene delivery vectors can effectively express the GFP reporter gene, delivering and expressing a large, fully functional gene construct is often a more difficult task. As a result, the efficacy of the gene therapy gel was evaluated by attempting to deliver a functional COL7A1 gene to RDEBK cells. Immunocytochemistry (ICC) was used to confirm the successful transfection of the cells using three different methods, as shown in Fig. S8. The transfected cells displayed a red fluorescence signal, indicating the presence of C7, while the negative control that was not treated showed no signal. Notably, the gene therapy gel group exhibited the highest expression of C7, which was consistent with the results observed in GFP pDNA transfected cells (Fig. 5a and Fig. S7). Although the in vitro trials have limitations, the successful transfection and expression of C7 in RDEBK cells, along with its potential for reduced toxicity, suggest that the gene therapy gel could be a promising alternative for gene therapy. Also, based on the proposed administration method for RDEB patients, the gene therapy gel will be applied on chronic wounds without the need of stratum corneum penetration. Thus, the polyplex released from the hydrogel will be able to transfect skin cells in the dermis directly, which reduces the difficulty of gene delivery. Another benefit of the gene therapy gel is that it may improve the safety of gene therapy by minimizing the leakage of functional polyplex into systemic blood circulation by controlled release and degradable gene delivery vectors. Furthermore, the gene therapy gel will help avoid wound dressing adherence, which is a common problem that causes pain and trauma during dressing changes for RDEB patients. The hydrogel can provide a moist and protective environment for wound healing while allowing easy removal of dressings [11]. However,

further optimization and in vivo testing are required to establish its safety and efficacy for clinical application.

4. Conclusion

Although diverse gene drug sustained-release systems have been previously reported, most of them are limited to the use of non-degradable polymers as vectors. Here, in contrast, a gene therapy gel was formulated by directly mixing granular hydrogels and polyplex nanoparticles prepared with degradable vectors and plasmid DNA. The results show the as-obtained gene therapy gel can modulate the release of polyplex nanoparticles, exhibiting reduced cytotoxicity and high long-term transfection levels. Moreover, depending on the applied load, the gene therapy gel can exhibit either “solid-like” or “liquid-like” rheological response, allowing rapid drug application to the lesion sites followed by efficient drug retention. Considering the delicate skin condition of RDEB patients and the need for daily dressing care, this combination of low toxicity, high efficacy, intrinsic lubricating properties, and ease of administration shows great potential for clinical translation of gene therapy gels as a new dosage form. In addition, vaccination against infectious respiratory diseases or alternative drug absorption methods, such as sublingual and buccal administration, can also potentially benefit from this granular hydrogel-mediated delivery process.

Ethics statement

The manuscript does not include any clinical trials. No ethics approval and consent to participate are required for this manuscript.

Data availability

The raw and processed data required to reproduce these findings are available from the corresponding authors upon request.

Declaration of competing interest

W.W. is the scientific founder and holds equity in Branca Bunús Ltd, a spin-out company of University College Dublin. L.P. is former employee in Branca Bunús Ltd. These interests have been fully disclosed to the University College Dublin and the approved plans are in place for managing any potential conflicts.

Acknowledgements

We thank Prof. Fernando Larcher (Centro de Investigaciones Energéticas, Medioambientales y Tecnológicas-CIEMAT, Madrid, Spain) for providing RDEB keratinocytes. This work was supported by National Key Research and Development Program of China (2021YFC2104300 to Ziyi Yu), the National Natural Science Foundation of China (21901117 to Ziyi Yu; 32111530117 to Ziyi Yu; 52003119 to Yu Shen; 52273207 to Jing Zhang; 81903240 to Ming Zeng) and Irish Research Council Government of Ireland Postdoctoral Fellowship Award (GOIPD/2020/788 to Zhonglei He). The authors also would like to acknowledge the support of Natural Science Foundation of Jiangsu Province (BK20221314 to Jing Zhang), State Key Laboratory of Materials-Oriented Chemical Engineering (SKL-MCE-22A06 to Ziyi Yu) and Clinical Frontier Technology Program of the First Affiliated Hospital of Jinan University (JNU1AF-CFTP-2022-a01230 to Ming Zeng).

References

1. S. Liu, Y. Gao, D. Zhou, M. Zeng, F. Alshehri, B. Newland, J. Lyu, J. O'Keeffe-Ahern, U. Greiser, T. Guo, F. Zhang, W. Wang Highly branched poly(β-amino ester) delivery of minicircle DNA for transfection of neurodegenerative disease related cells Nat. Commun., 10 (2019), p. 3307
2. J. O'Keeffe Ahern, I. Lara-Saez, D. Zhou, R. Murillas, J. Bonafont, Á. Mencía, M. García, D. Manzanares, J. Lynch, R. Foley, Q. Xu, A. Sigen, F. Larcher, W. Wang Non-viral delivery of CRISPR–Cas9 complexes for targeted gene editing via a polymer delivery system Gene. Ther., 29 (2022), pp. 157-170
3. J. Li, X. Li, Y. Zhang, X.K. Zhou, H.S. Yang, X.C. Chen, Y.S. Wang, Y.Q. Wei, L.J. Chen, H.Z. Hu, C.Y. Liu Gene therapy for psoriasis in the K14-VEGF transgenic mouse model by topical transdermal delivery of interleukin-4 using ultradeformable cationic liposome J Gene Med, 12 (2010), pp. 481-490
4. A.K. Patel, J.C. Kaczmarek, S. Bose, K.J. Kauffman, F. Mir, M.W. Heartlein, F. DeRosa, R. Langer, D.G. Anderson Inhaled nanoformulated mRNA polyplexes for protein production in lung epithelium Adv. Mater., 31 (2019), Article 1805116
5. J. Rosenecker, S. Huth, C. Rudolph Gene therapy for cystic fibrosis lung disease: current status and future perspectives Curr. Opin. Mol. Ther., 8 (2006), pp. 439-445
6. Badea, S. Wettig, R. Verrall, M. Foldvari Topical non-invasive gene delivery using gemini nanoparticles in interferon-γ-deficient mice Eur. J. Pharm. Biopharm., 65 (2007), pp. 414-422
7. S. Alqawlaq, J.M. Sivak, J.T. Huzil, M.V. Ivanova, J.G. Flanagan, M.A. Beazely, M. Foldvari Preclinical development and ocular biodistribution of gemini-DNA nanoparticles after intravitreal and topical administration: towards non-invasive glaucoma gene therapy Nanomed. Nanotechnol. Biol. Med., 10 (2014), pp. 1637-1647
8. W. Chen, H. Li, D. Shi, Z. Liu, W. Yuan Microneedles as a delivery system for gene therapy Front. Pharmacol., 7 (2016), p. 137
9. C. Li, Y. Du, H. Lv, J. Zhang, P. Zhuang, W. Yang, Y. Zhang, J. Wang, W. Cui, W. Chen Injectable amphipathic artesunate prodrug-hydrogel microsphere as gene/drug nano-microplex for rheumatoid arthritis therapy Adv. Funct. Mater., 32 (2022), Article 2206261
10. Y. Cao, Z. He, Q. Chen, X. He, L. Su, W. Yu, M. Zhang, H. Yang, X. Huang, J. Li Helper-polymer based five-element nanoparticles (FNPs) for lung-specific mRNA delivery with long-term stability after lyophilization Nano Lett, 22 (2022), pp. 6580-6589
11. Gurevich, P. Agarwal, P. Zhang, J.A. Dolorito, S. Oliver, H. Liu, N. Reitze, N. Sarma, I.S. Bagci, K. Sridhar, V. Kakarla, V.K. Yenamandra, M. O'Malley, M. Prisco, S.F. Tufa, D.R. Keene, A.P. South, S.M. Krishnan, M.P. Marinkovich In vivo topical gene therapy for recessive dystrophic epidermolysis bullosa: a phase 1 and 2 trial Nat. Med., 28 (2022), pp. 780-788
12. N. Ahmad, M. Pandey, N. Mohamad, X.Y. Chen, M.C.I.M. Amin In Targeting Chronic Inflammatory Lung Diseases Using Advanced Drug Delivery Systems Academic Press (2020) Ch. 21
13. T.H. Qazi, J. Wu, V.G. Muir, S. Weintraub, S.E. Gullbrand, D. Lee, D. Issadore, J.A. Burdick Anisotropic rod-shaped particles influence injectable granular hydrogel properties and cell invasion Adv. Mater., 34 (2022), Article 2109194
14. W. Cheng, J. Zhang, J. Liu, Z. Yu Granular hydrogels for 3D bioprinting applications View, 1 (2020), Article 20200060
15. J. Zhang, Y. Qin, Y. Ou, Y. Shen, B. Tang, X. Zhang, Z. Yu Injectable granular hydrogels as colloidal assembly microreactors for customized structural colored objects Angew. Chem. Int. Ed., 61 (2022), Article e202206339
16. H.S. Jung, K.S. Kim, S.H. Yun, S.K. Hahn Enhancing the transdermal penetration of nanoconstructs: could hyaluronic acid be the key? Nanomedicine, 9 (2014), pp. 743-745
17. S.B. Shibata, S.R. Cortez, J.A. Wiler, D.L. Swiderski, Y. Raphael Hyaluronic acid enhances gene delivery into the cochlea Hum. Gene Ther., 23 (2012), pp. 251-335

18. J. Zhang, Y. Qin, O.J. Pambos, J. Zhang, S. Chen, Z. Yu, C. Abell Microdroplets confined assembly of opal composites in dynamic borate ester-based networks Chem. Eng. J., 426 (2021), Article 127581
19. H. Wang, Z. Zhao, Y. Liu, C. Shao, F. Bian, Y. Zhao Biomimetic enzyme cascade reaction system in microfluidic electrospray microcapsules Sci. Adv., 4 (2018), p. eaat2816
20. W. Leong, T.T. Lau, D.A. Wang A temperature-cured dissolvable gelatin microsphere-based cell carrier for chondrocyte delivery in a hydrogel scaffolding system Acta Biomater., 9 (2013), pp. 6459-6467
21. T. Yuan, Y. Li, D.P. Song Interfacial self-assembly of amphiphilic core-shell bottlebrush block copolymers toward responsive photonic balls bearing ionic channels Macromol. Rapid Commun., 43 (2022), Article 2200188
22. S.M. Naqvi, S. Vedicherla, J. Gansau, T. McIntyre, M. Doherty, C.T. Buckley Living cell factories - electrosprayed microcapsules and microcarriers for minimally invasive delivery Adv. Mater., 28 (2016), pp. 5662-5671
23. A.C. Daly, L. Riley, T. Segura, J.A. Burdick Hydrogel microparticles for biomedical applications Nat. Rev. Mater., 5 (2020), pp. 20-43
24. N. Segovia, M. Pont, N. Oliva, V. Ramos, S. Borrós, N. Artzi Hydrogel dopped with nanoparticles for local sustained release of siRNA in breast cancer Adv. Healthc. Mater., 4 (2015), pp. 271-280
25. J.A. Duran-Mota, J.Q. Yani, B.D. Almquist, S. Borrós, N. Oliva Polyplex-loaded hydrogels for local gene delivery to human dermal fibroblasts ACS Biomater. Sci. Eng., 7 (2021), pp. 4347-4361
26. Y. He, G. Cheng, L. Xie, Y. Nie, B. He, Z. Gu Polyethyleneimine/DNA polyplexes with reduction-sensitive hyaluronic acid derivatives shielding for targeted gene delivery Biomaterials, 34 (2013), pp. 1235-1245
27. E. Kurt, T. Segura Nucleic acid delivery from granular hydrogels Adv. Health. Mater., 11 (2022), Article 2101867
28. T.F. Martens, K. Remaut, H. Deschout, J.F.J. Engbersen, W.E. Hennink, M.J. van Steenbergen, J. Demeester, S.C.D. Smedt, K. Braeckmans Coating nanocarriers with hyaluronic acid facilitates intravitreal drug delivery for retinal gene therapy J. Control. Release, 202 (2015), pp. 83-92
29. K. Urbiola, C. Sanmartín, L. Blanco-Fernández, C.T. de Ilarduya Efficient targeted gene delivery by a novel PAMAM/DNA dendriplex coated with hyaluronic acid Nanomedicine, 9 (2014), pp. 2787-2801
30. D. Veilleux, R.K.G. Panicker, A. Chevrier, K. Biniecki, M. Lavertu, M.D. Buschmann Lyophilisation and concentration of chitosan/siRNA polyplexes: influence of buffer composition, oligonucleotide sequence, and hyaluronic acid coating J. Colloid Interface Sci., 512 (2018), pp. 335-345
31. A.V. Oliveira, D.B. Bitoque, G.A. Silva Combining hyaluronic acid with chitosan enhances gene delivery J. Nanomater., 2014 (2014), p. 152
32. M. Zeng, Q. Xu, D.Z. Zhou, A. Sigen, F. Alshehr, I. Lara-Sáez, Y. Zheng, M. Li, W. Wang Highly branched poly(β-amino ester)s for gene delivery in hereditary skin diseases Adv. Drug Deliv. Rev., 176 (2021), Article 113842
33. D.M. Lynn, R. Langer Degradable poly(β-amino esters): synthesis, characterization, and self-assembly with plasmid DNA J. Am. Chem. Soc., 122 (2000), pp. 10761-10768
34. D. Zhou, L. Cutlar, Y. Gao, W. Wang, J. O'Keeffe-Ahern, S. McMahon, B. Duarte, F. Larcher, B.J. Rodriguez, U. Greiser, W. Wang The transition from linear to highly branched poly(β-amino ester)s: branching matters for gene delivery Sci. Adv., 2 (2016), Article e1600102
35. M. Zeng, D. Zhou, F. Alshehri, I. Lara-Sáez, Y. Lyu, J. Creagh-Flynn, Q. Xu, S. A, J. Zhang, W. Wang Manipulation of transgene expression in fibroblast cells by a multifunctional linear-

branched hybrid poly(β-amino ester) synthesized through an oligomer combination approach Nano Lett., 19 (2019), pp. 381-391

36. C. Chamorro, D. Almarza, B. Duarte, S.G. Llames, R. Murillas, M. García, J.C. Cigudosa, L. Espinosa-Hevia, M.J. Escámez, Á. Mencía, Á. Meana, R. García-Escudero, R. Moro, C.J. Conti, M.D. Río, F. Larcher Keratinocyte cell lines derived from severe generalized recessive Epidermolysis Bullosa patients carrying a highly recurrent COL7A1 homozygous mutation: models to assess cell and gene therapies in vitro and in vivo Exp. Dermatol., 22 (2013), pp. 601-603

Supporting Information

Enhanced Gene Transfection Efficacy and Safety through Granular Hydrogel Mediated Gene Delivery Process

Jing Zhang, Zhonglei He, Yinghao Li, Yu Shen, Guanfu Wu, Laura Power, Rijian Song, Ming Zeng, Xianqing Wang, Irene Lara Sáez, Sigen A, Qian Xu, James F. Curtin, Ziyi Yu, and Wenxin Wang***

* Corresponding author. State Key Laboratory of Materials-Oriented Chemical Engineering, College of Chemical Engineering, Nanjing Tech University, 30 Puzhu South Road, Nanjing, 211816 P. R. China.

** Corresponding author. Research and Clinical Translation Center of Gene Medicine and Tissue Engineering, School of Public Health, Anhui University of Science and Technology, Huainan, 232001, China & Charles Institute of Dermatology, School of Medicine, University College Dublin, Dublin, Ireland.

E-mail addresses: ziyi.yu@njtech.edu.cn (Z. Yu); wwxph@aust.edu.cn, wenxin.wang@ucd.ie (W. Wang).

Supporting Figures

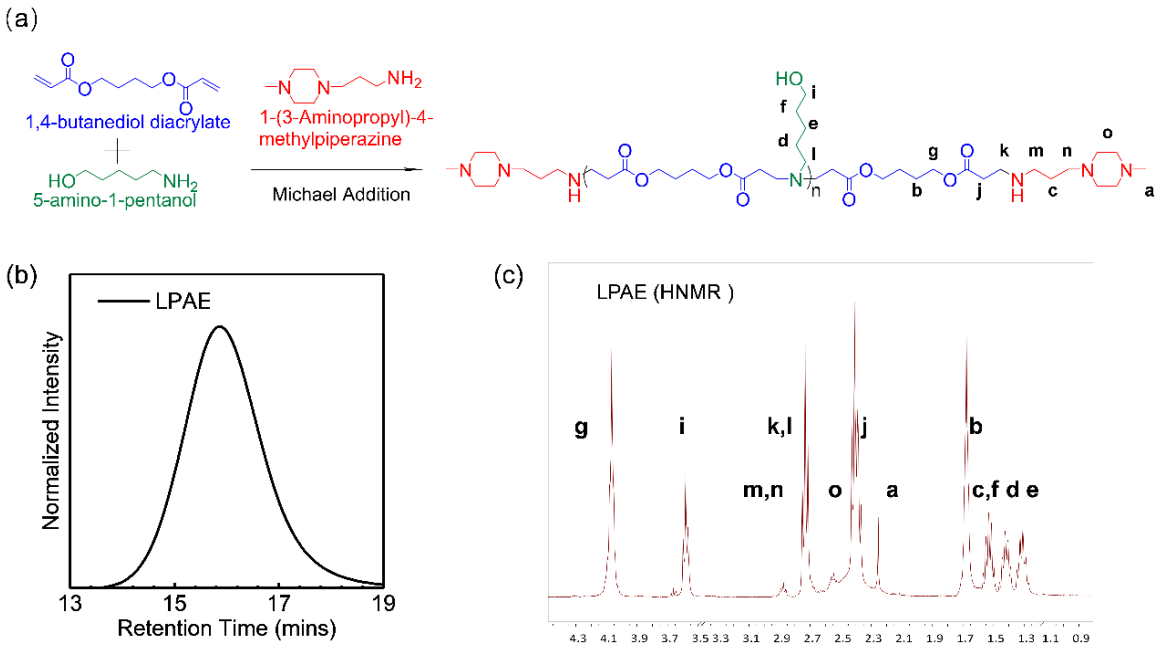

Fig. S1. (a) An illustration of the process for synthesizing LPAE. (b) The GPC trace of the LPAE polymer synthesized in this study. (c) The ^{1}H NMR analysis of the LPAE polymer.

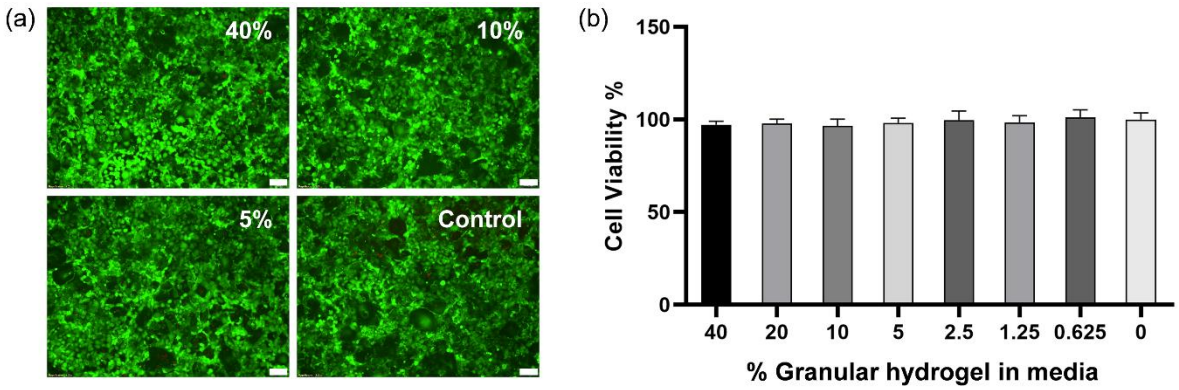

Fig. S2. Both live/dead staining (a) and the Alamar Blue cell viability assay (b) have provided evidence of minimal cytotoxicity in the granular hydrogels that make up the gene therapy gels. The COS7 cell line was subjected to live/dead staining after exposure to different volume ratios of granular hydrogel to culture media, ranging from 0% (the control) to 40%. Scale bar = 100 μm.

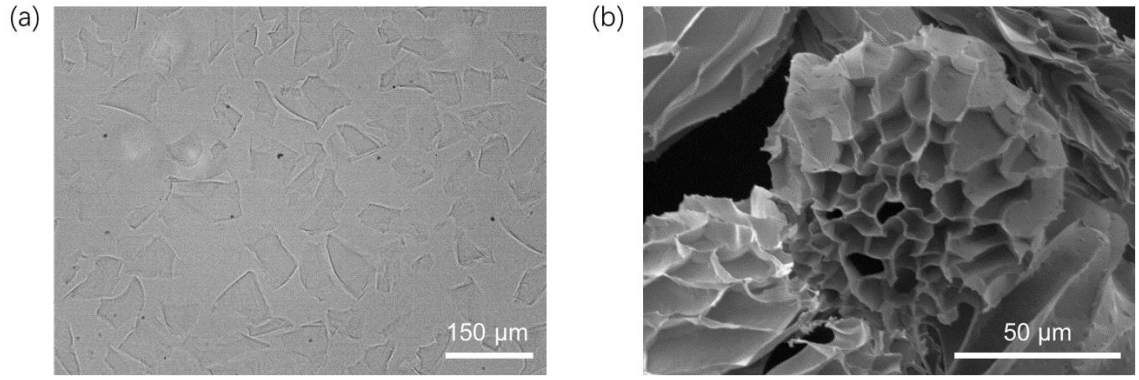

Fig. S3. The resulting HMPs with a mean size of 120 µm as captured by (a) a microscope image and (b) a scanning electron microscope (SEM) image

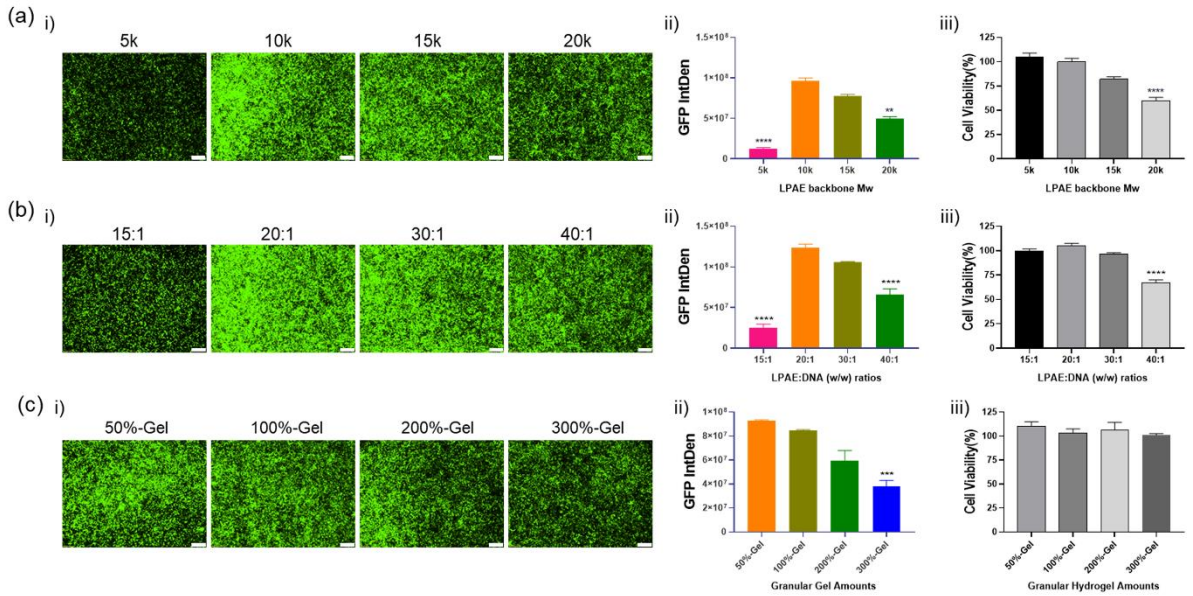

Fig. S4. The influence of different variables, including the molecular weight of LPAE polymers, LPAE polymer to DNA weight ratios, and polyplex nanoparticles to granular hydrogel weight-volume ratios on the transfection efficiency of HEK293 cells (a) HEK293 cells were transfected using LPAE polymers with different molecular weights, while keeping the LPAE polymer to DNA weight ratio constant at 20:1. (b) HEK293 cells were transfected with polyplex nanoparticles generated at various polymer to DNA weight ratios utilizing LPAE with a molecular weight of approximately 10 kDa. (c) Transfection of HEK293 cells was achieved using gene therapy gels with varied weight-volume ratios of polyplex nanoparticles and granular hydrogel. The gels were created by mixing lyophilized polyplex nanoparticles with 1 mL of granular hydrogel to produce DNA concentrations of 2.5, 5, 10, and 15 µg/mL, designated as 50%-Gel, 100%-Gel, 200%-Gel, and 300%-Gel, respectively. To enable successful cell transfection, it was crucial to evenly distribute an equivalent amount of plasmid DNA (i.e., 0.5 µg per well) consistently across all 96 wells. Moreover, LPAE polymer with an estimated molecular weight of 10 kDa was selected, and a constant weight ratio of 20:1 between the LPAE polymer and DNA was maintained. Scale bar = 200 µm.

Our research investigated how several factors impact the transfection efficiency of HEK293 cells, including the molecular weight of LPAE polymers, the weight ratios of LPAE polymer to DNA, and the weight-volume ratios of polyplex nanoparticles to granular hydrogel. As shown in Fig. S4a, the LPAE polymer with a molecular weight of approximately 5 kDa had limited effectiveness. However, the LPAEs with higher molecular weights of 15 and 20 kDa showed an improvement in overall GFP expression, although they also resulted in greater cytotoxicity compared to the 10 kDa LPAE. The findings indicate that the instability and limited DNA capturing ability of small molecular weight LPAE may make it less efficient as a gene vector, while larger polymer molecules may have higher cytotoxicity due to their difficulty in breaking

down. As a result, for the preparation of polyplex nanoparticles, the 10 kDa PAE was chosen as the vector, unless specified otherwise in the study.

Based on Fig. S4b, it was found that using the 10 kDa LPAE as the vector, a low weight ratio of polymer to DNA (15:1) led to insufficient transfection efficiency, whereas high weight ratios (30:1 and 40:1) resulted in a slight rise in cytotoxicity and reduced GFP expression. As a result, a weight ratio of 20:1 was ultimately chosen for the subsequent experiment in this study. Figure S4c indicates that a decrease in the weight-volume ratios of polyplex nanoparticles to granular hydrogel leads to a decrease in transfection efficiency. This decline in efficiency is likely due to the excess hydrogel microparticles (HMPs), which strongly bond with polyplex nanoparticles via electrical attraction and increase the distance that polyplex nanoparticles must travel, resulting in a reduced release rate. This may cause many polyplex nanoparticles to degrade before entering transfected cells, resulting in a loss of efficacy. Additionally, it is worth mentioning that increasing the amount of granular hydrogels used in the transfection process did not result in significant cytotoxicity, further confirming the biocompatibility of the granular hydrogels used in the experiment.

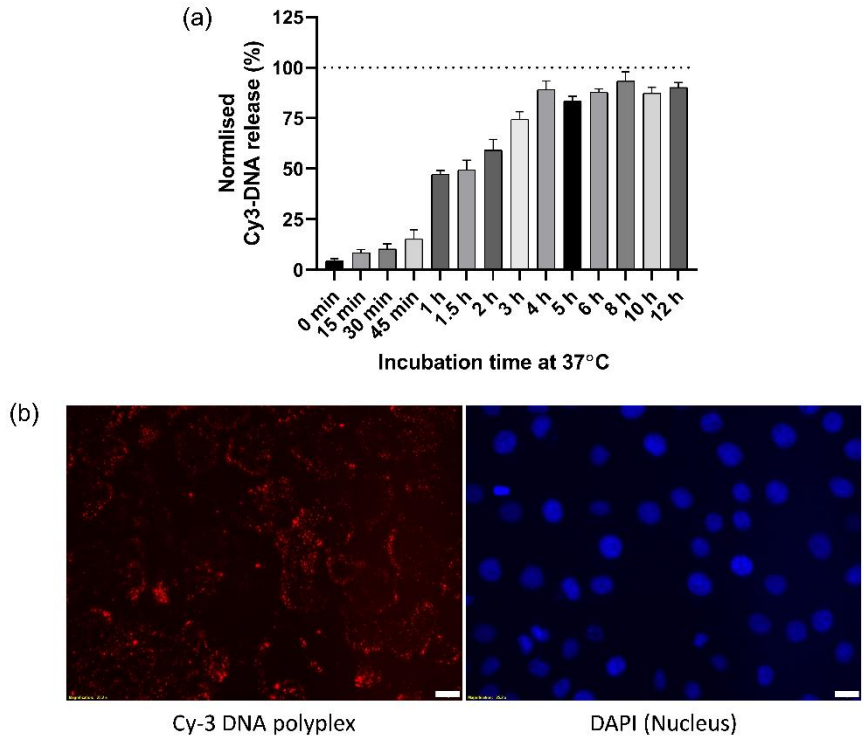

Fig. S5. Examination of the discharge kinetics of Cy3-DNA/LPAE polyplex nanoparticles from the gene therapy hydrogel (a) The method used to evaluate the liberation of Cy3-DNA/LPAE polyplex nanoparticles from the gene therapy gel involved comparing the fluorescence intensity of the release solution with that of a freely dispersed polyplex nanoparticle solution with equivalent Cy3-DNA concentration. (b) The gene therapy gel was used to transfected RDEBK cells, and intracellular imaging of Cy3-DNA/LPAE polyplex nanoparticles was conducted four hours after transfection. Scale bar = 20 µm.

Fig. S5a demonstrates that the gene therapy gel effectively captured more than 90% of the polyplex nanoparticles and modulated their release during transfection. Although the release rate was initially slow within the first 45 minutes of incubation in PBS, it markedly accelerated after 1 hour, and most of the nanoparticles were released after 4 hours. This optimized release process can reduce cytotoxicity while preserving the efficacy of the polyplex nanoparticles before they enter the cells, which is supported by the results shown in Fig. 4.

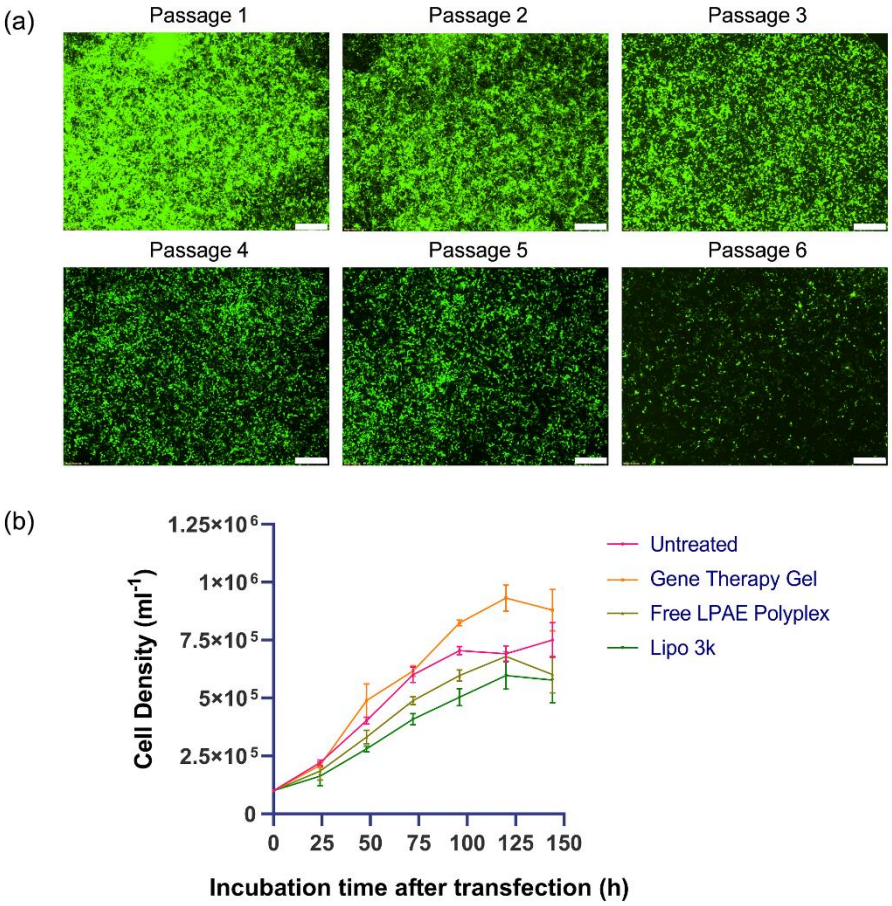

Fig. S6. Long term GFP expression and growth rate studies after transfection of HEK293 cells (a) The sustained expression of GFP in HEK293 cells following a single transfection with the gene therapy gel over an extended period. Scale bar = 200 µm. (b) To assess the impact of the transfection method on cell growth, the growth rate of HEK293 cells was compared under four conditions: untreated control group, free LPAE polyplex group (representing free LPAE-pDNA polyplex nanoparticles transfected), gene therapy gel group, and Lipo3k group (representing free Lipo3k-pDNA lipid nanoparticles transfected).

Fig. S6a illustrates the evaluation of long-term GFP expression in the optimal transfection condition using gene therapy gel. Initially, the GFP signal decreased following the first subculture, which may be due to the distribution of transfected pDNA and expressed GFP from mother-cells to daughter-cells. Passage 1 was imaged 48 hours after transfection, while passage 2 was imaged 72 hours after transfection and 24 hours after the first subculture. The signal remained relatively constant between passages 2 and 3, and passages 4 and 5, perhaps due to a balance between moderate increase and accumulation of GFP expression and cell division. However, by passage 6, most GFP expression was lost.

In the study, cell density was monitored to determine the growth rate of HEK293 cells under various transfection conditions. The cells were cultured in individual wells and the medium

was changed every two days. At each time point, cell density was measured in three wells from each group. The results indicated that the cell growth rates were consistent with the cell viability assay, as demonstrated in Fig. 4b. The untreated and gene therapy gel transfected groups showed the highest cell growth rates with doubling times of approximately 26-28 hours, while Lipo 3K and free polyplex exhibited cell growth inhibition and cytotoxicity, resulting in a decrease in growth rate and doubling times of around 30-33 hours, as shown in Fig. S6b.

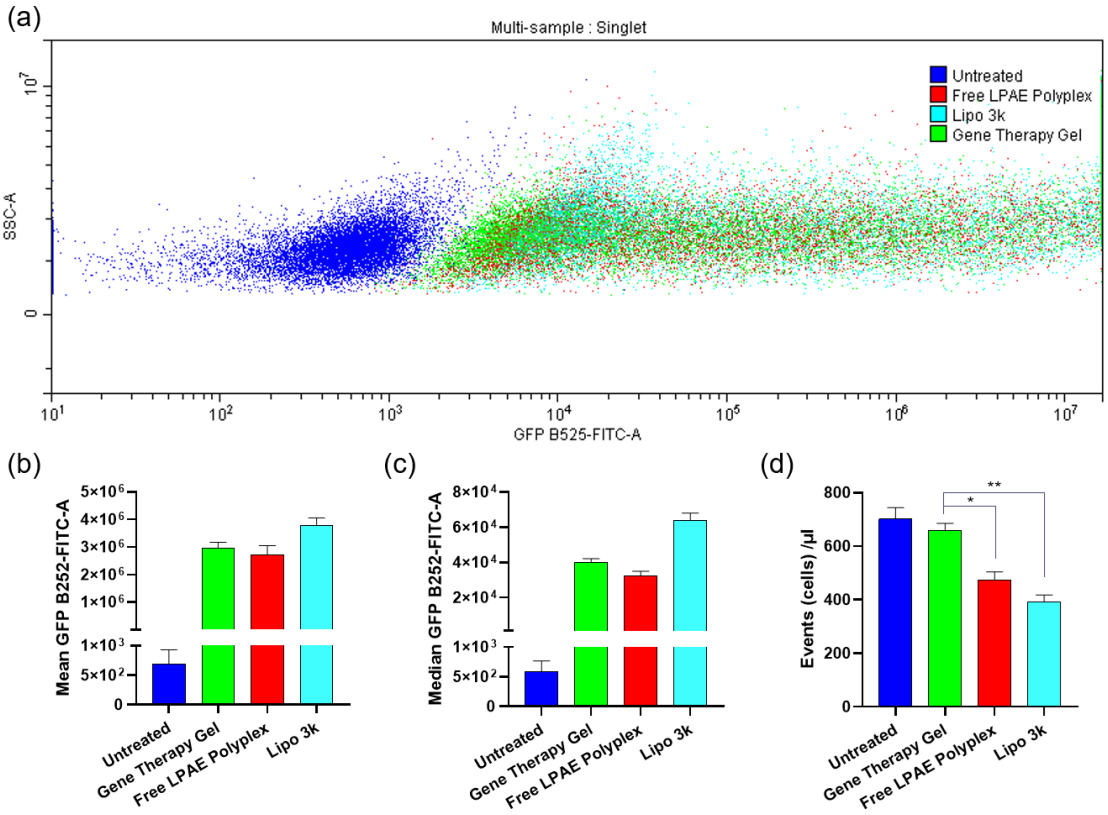

Fig. S7. Flow cytometric analysis of RDEBK cells after transfection (a) The dot plot depicts single-cell data for four distinct experimental conditions: the untreated control, the free LPAE polyplex group, the gene therapy gel group, and the Lipo 3k group. The mean (b) and median (c) fluorescence intensity of GFP were calculated for four selected groups. All three transfected groups had similar average GFP intensity, with the Lipo3k transfected group having a slightly higher median. (d) The cell density (singlet events/µL) for each group was measured to evaluate post-transfection cell viability. The results showed that the gene therapy gel transfected group had the highest cell density, followed by the free polyplex transfected group and then the Lipo3k transfected group. Statistical analysis indicated that the differences between the groups were significant (* $p < 0.05$, ** $p < 0.01$).

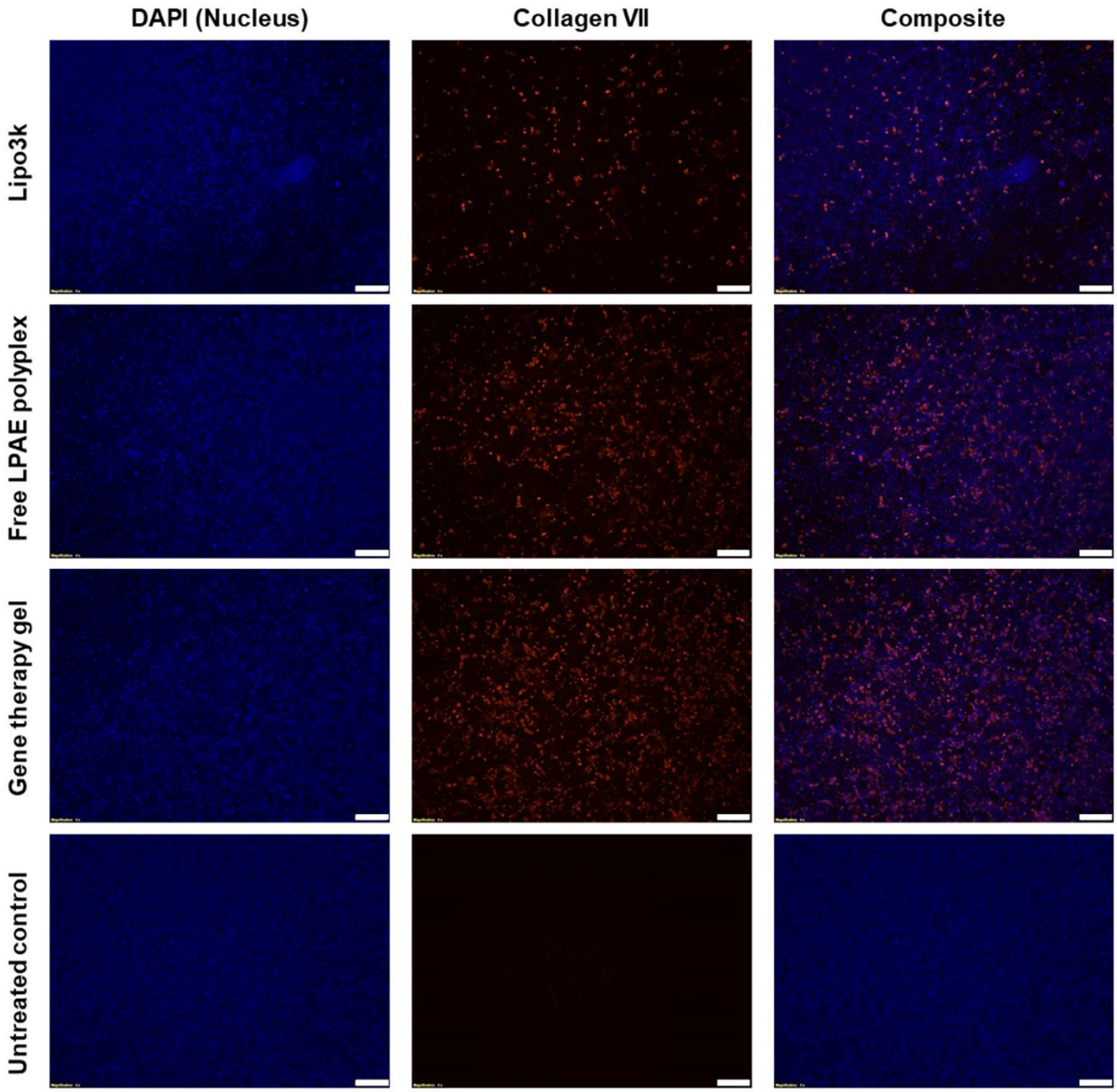

Fig. S8. Immunocytochemistry (ICC) imaging was performed on RDEBK cells to evaluate collagen VII protein (C7) expression after transfection using three different conditions: Lipo 3k group, free LPAE polyplex group, and gene therapy gel group. The ICC images illustrate the selective staining of C7 in RDEBK cells, indicated by the distinguishable red fluorescence signal. The specificity of the staining was verified by the lack of signal in the negative untreated control. Scale bar = 200 µm.